BRASSINOSTEROID INSENSITIVE2 negatively regulates cellulose synthesis in *Arabidopsis* by phosphorylating cellulose synthase 1

Clara Sánchez-Rodríguez[a,1], KassaDee Ketelaar[b,1], Rene Schneider[c], Jose A. Villalobos[b], Chris R. Somerville[d,2], Staffan Persson[c,2,3], and Ian S. Wallace[b,2,3]

[a]Department of Biology, Eidgenössiche Technische Hochschule Zurich, 8092 Zurich, Switzerland; [b]Department of Biochemistry and Molecular Biology, University of Nevada, Reno, NV 89557; [c]School of Biosciences, University of Melbourne, Parkville 3010, VIC, Australia; and [d]Energy Biosciences Institute, University of California, Berkeley, CA 94720

Contributed by Chris R. Somerville, February 12, 2017 (sent for review September 7, 2016; reviewed by Steve C. Huber and Simon R. Turner)

The deposition of cellulose is a defining aspect of plant growth and development, but regulation of this process is poorly understood. Here, we demonstrate that the protein kinase BRASSINOSTEROID INSENSITIVE2 (BIN2), a key negative regulator of brassinosteroid (BR) signaling, can phosphorylate *Arabidopsis* cellulose synthase A1 (CESA1), a subunit of the primary cell wall cellulose synthase complex, and thereby negatively regulate cellulose biosynthesis. Accordingly, point mutations of the BIN2-mediated CESA1 phosphorylation site abolished BIN2-dependent regulation of cellulose synthase activity. Hence, we have uncovered a mechanism for how BR signaling can modulate cellulose synthesis in plants.

plant cell wall | brassinosteroid | cellulose synthase | protein kinase | regulation

Plant growth is controlled by a plethora of intra- and extracellular processes; however, the major driving force for plant cell growth stems from changes in vacuolar turgor pressure that modulate cell volume. Because all plant cells are encased in cell walls, plant cell expansion is also dependent on synthesis and remodeling of cell wall polysaccharides, including cellulose (1). Cellulose is the most abundant biopolymer on Earth and is a fundamental constituent of plant cell walls. This paracrystalline polysaccharide is synthesized at the plasma membrane by cellulose synthase A (CESA) complexes (CSCs) (2). Current models suggest that the CSC is a heterotrimeric complex in which CESA1-, CESA3-, and CESA6-like CESAs are involved in primary wall cellulose synthesis in *Arabidopsis thaliana* (3, 4). Nascent cellulose chains are incorporated into the cell wall matrix, and additional synthesis pushes the CSC through the plasma membrane (5), which was confirmed by motile fluorescently labeled CESA proteins at the plasma membrane (6). Nevertheless, the regulation of CSC activity remains largely ill defined.

Phytohormones control plant growth and development. Among these hormones, brassinosteroids (BRs) are particularly important for normal plant cell expansion. BRs are perceived at the plasma membrane by the receptor-like kinase BRASSINOSTEROID INSENSITIVE1 (BRI1), which activates a signal transduction cascade, leading to the transcriptional regulation of BR-responsive genes (7, 8). A key regulator in BR signaling is the glycogen synthase kinase 3 (GSK3)-like BRASSINOSTEROID INSENSITIVE2 (BIN2) (9). In the absence of BRs, BIN2 is active and phosphorylates the two homologous transcription factors, BRASSINAZOLE RESISTANT1 (BZR1) and BZR2/BES1 (10, 11), which results in their inactivation and degradation. In contrast, when BR is present, BIN2 is inactivated and degraded (12), which leads to activation of BZR1 and BZR2/BES1, and therefore to transcriptional activation of BR-responsive genes. Thus, BIN2 serves as a key negative regulator of BR-mediated transcriptional responses. However, additional targets of BIN2 kinase and their role in the regulation of cell expansion remain to be elucidated.

Considering the importance of cell wall synthesis and environmental signaling for plant growth, close links between these processes have been postulated (13). For example, live-cell imaging has revealed that CSC speed is regulated by the red light/far-red light ratio in a PHYTOCHROME B (PHYB)-dependent manner, and this regulation was proposed to be mediated through CESA5 phosphorylation (14). Additionally, the BR-regulated BZR1/BES1 transcriptional activators directly bind the promoters of *CESA* genes involved in cellulose biosynthesis of the primary and secondary cell walls (15). However, more direct associations between CSC activity and BR signaling remain tenuous. Here, we show that BIN2 can phosphorylate CESA1 and that this phosphorylation negatively regulates CSC activity.

Results

Defects in BR Synthesis and Signaling Impair Cellulose Synthesis. Previous work has demonstrated a potential relationship between BR signal transduction and the transcriptional regulation of *CESA* genes (15). To investigate the influence of BR signaling on cellulose synthesis in more detail, we first analyzed crystalline cellulose content in BR-deficient seedlings via the Updegraff assay. We found that mutations in *DET2* (*det2-1*; a key enzyme in BR synthesis) (16) or a hypermorphic mutation in *BIN2* that renders BIN2 constitutively active (*bin2-1*) (9) negatively impacted crystalline cellulose content in

Significance

Cellulose is the most abundant biopolymer on Earth and is a critical component for plants to grow and develop. Cellulose is synthesized by large cellulose synthase complexes containing multiple cellulose synthase A (CESA) subunits; however, how cellulose synthesis is regulated remains unclear. In this study, we identify BRASSINOSTEROID INSENSITIVE2 (BIN2) as a protein kinase that directly phosphorylates *Arabidopsis* CESA1 and further demonstrate that this phosphorylation event negatively regulates CESA activity, and thus cellulose biosynthesis, in *Arabidopsis*. Therefore, this study provides a clear link between cell wall biosynthesis and hormonal signal transduction pathways that regulate plant growth and development.

Author contributions: C.S.-R., R.S., C.R.S., S.P., and I.S.W. designed research; C.S.-R., K.K., R.S., J.A.V., and I.S.W. performed research; I.S.W. contributed new reagents/analytic tools; C.S.-R., K.K., R.S., J.A.V., C.R.S., S.P., and I.S.W. analyzed data; and C.S.-R., K.K., R.S., C.R.S., S.P., and I.S.W. wrote the paper.

Reviewers: S.C.H., University of Illinois; and S.R.T., University of Manchester.

The authors declare no conflict of interest.

[1]C.S.-R. and K.K. contributed equally to this work.

[2]To whom correspondence may be addressed. Email: crs@berkeley.edu, staffan.persson@unimelb.edu.au, or iwallace@unr.edu.

[3]S.P. and I.S.W. contributed equally to this work.

This article contains supporting information online at www.pnas.org/lookup/suppl/doi:10.1073/pnas.1615005114/-/DCSupplemental.

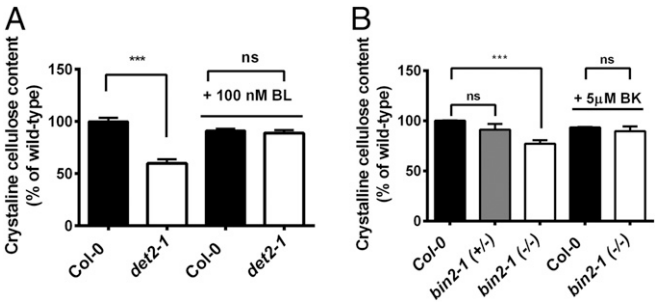

Fig. 1. Cellulose biosynthesis depends on BR synthesis and signaling. The crystalline cellulose content of 5-d-old dark-grown seedlings was analyzed as described in *Materials and Methods*. (*A*) Crystalline cellulose content of wild-type Col-0 (black bars) and *det2-1* (white bars) seedlings grown in the presence or absence of 100 nM eBL. (*B*) Similar analyses were performed for *bin2-1* heterozygous (*bin2-1*$^{+/-}$; gray bars) and homozygous (*bin2-1*$^{-/-}$; white bars) mutants in the presence or absence of 5 μM bikinin (BK). Crystalline cellulose contents are reported as a percentage of the crystalline cellulose content of wild-type untreated controls. Error bars for both *A* and *B* represent SEM (n = 3 biological replicates per biological replicate, n = 2 technical replicates per biological replicate; ***$P < 0.005$ by Student's t test). ns, not significant by Student's t test.

etiolated seedlings compared with wild-type seedlings (Fig. 1 *A* and *B*). Furthermore, etiolated *det2-1* seedlings grown on media supplemented with epibrassinolide (eBL; 100 nM) restored the crystalline cellulose content to wild-type levels (Fig. 1*A*). Likewise, the crystalline cellulose content was restored to wild-type levels in *bin2-1* seedlings grown on bikinin (5 μM; a potent BIN2 inhibitor) (17) (Fig. 1*B*). These data indicate that changes in BR synthesis and signaling impact the production of crystalline cellulose.

To investigate the relationship between cellulose synthesis and BR in more detail, we introgressed a transgenic *YFP-CESA6* fluorescent reporter under the control of the *CESA6* native promoter (6) into the *det2-1* or *bin2-1* mutant background. Previous studies have demonstrated that the speed of the CSC at the plasma membrane indicates cellulose synthase activity (6, 18–21). Hence, we investigated the CSC motility using time-averaged projections of CSC trajectories collected by spinning disk microscopy in *det2-1* and *bin2-1* and compared those trajectories with the trajectories of wild-type control (Fig. 2 *A* and *B*). The speeds of the CSCs were reduced by ∼20% in the *det2-1* background (13 cells, seven seedlings, 790 particles), and treatment of exogenous eBL (10 nM for 30 min; 12 cells, six seedlings, 954 particles) significantly increased the CSC speeds in *det2-1* (Fig. 2 *B* and *C*). Similarly, the CSC speeds were reduced by 40% in the *bin2-1* mutant compared with wild-type control (*YFP-CESA6*: five cells, five seedlings, 330 particles; *bin2-1*: 14 cells, seven seedlings, 1,100 particles; Fig. 2 *B* and *C*). Furthermore, the speeds of the CSCs were significantly increased (eight cells, eight seedlings, 546 particles) in *bin2-1* seedlings treated with bikinin (5 μM for 40 min) compared with control-treated *bin2-1* seedlings (Fig. 2 *B* and *C*). Wild-type Col-0 plants treated with 10 nM eBL for 30 min did not exhibit increased *CESA1* transcript levels (Fig. S1*A*). In contrast, both the *bin2-1* mutant and the *bin2-1* mutant treated with 5 μM BK had slightly higher transcript levels of *CESA1* compared with control seedlings (Fig. S1*B*). Nevertheless, because CSC speeds were significantly reduced in *bin2-1*, it appears that the changes in *CESA1* transcripts do not relate directly to CSC speeds. These data indicate that reduced BR synthesis in *det2-1* or increased BIN2 activity in the constitutively active *bin2-1* negatively impacts cellulose synthesis in *Arabidopsis* seedlings.

The BIN2 Protein Kinase Can Phosphorylate *Arabidopsis* CESA1. Genes that are transcriptionally coexpressed with the *CESA*s typically impact cellulose biosynthesis (22). To assess if any BR-related genes that could potentially influence cellulose biosynthesis were coexpressed with the *CESA*s, we used the recently developed FamNet (23) with several primary wall cellulose-related genes as queries, including *CESA1*, *CESA6*, the CSC-associated KORRIGAN 1 (*KOR1*) endoglucanase (24, 25), the GPI-anchored *COBRA* (26, 27), and the companion of cellulose synthase 1 (*CC1*) (28). Interestingly, we found that *BIN2* was coexpressed with many of the primary wall cellulose-related genes (Fig. S2), suggesting that BIN2 might influence cellulose production, potentially through its protein kinase activity. Many CSC subunits can become phosphorylated at multiple positions (29–32), and some of these phosphorylation events have been demonstrated to regulate the CSC functionally (14, 33, 34). However, the corresponding protein kinases have remained unidentified.

To test the hypothesis that BIN2 directly phosphorylates a component of the CSC, we produced synthetic peptides (Table

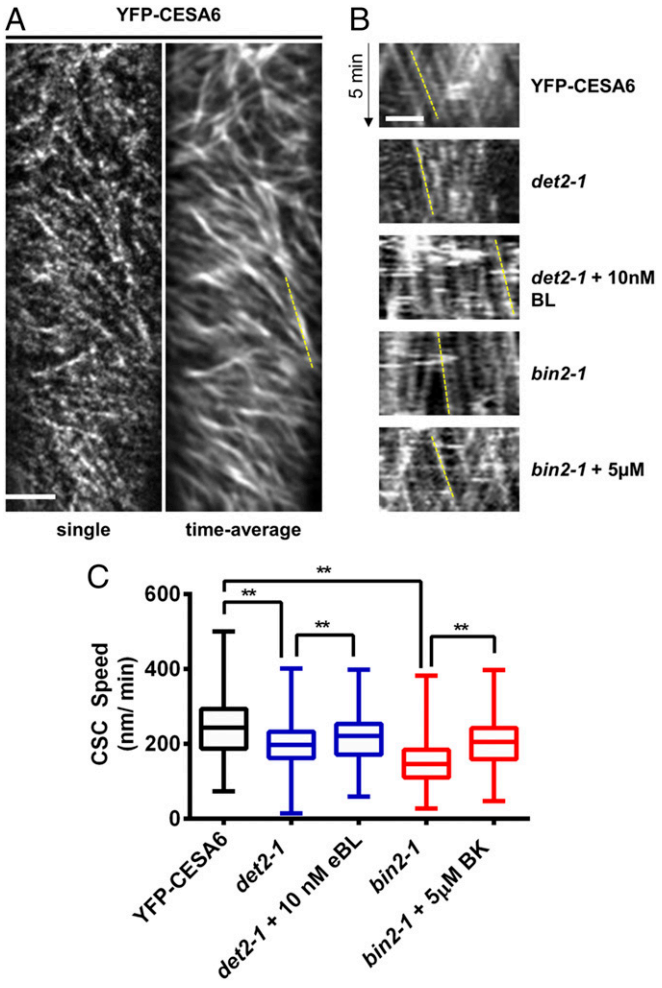

Fig. 2. CSC speeds are altered in BR mutants. CSC speeds were examined in 4-d-old dark-grown seedlings by spinning disk microscopy. (*A*) Single-frame and time-averaged images of YFP-CESA6 control seedlings. (Scale bar: 5 μm.) (*B*) Kymographs of YFP-CESA6 are shown for the indicated genotype and treatment. The dashed yellow line indicates the slope of a representative YFP-CESA6–containing particle. (Scale bar: 5 μm.) (*C*) YFP-CESA6 speed distributions of *det2-1* plus or minus 10 nM brassinolide (BL; blue boxes) and *bin2-1* (red boxes) seedlings plus or minus 5 μM BK are shown compared with YFP-CESA6 control seedlings. Treatments were performed at the indicated concentration for 30 min before imaging. Error bars represent minimum and maximum values (n = 324–1,100 particles). One-way ANOVA indicated a significant difference: $F(4, 3{,}681) = 249.5$ (**$P < 0.01$ by Tukey post hoc analysis between the indicated conditions).

S1) that corresponded to all reported phosphorylation sites in several cellulose-related proteins in *Arabidopsis*, including CESA1, CESA3, and CESA5, as well as KOR1 (29–32). BIN2 is a member of the GSK3-like kinase family, whose members can recognize substrates by either forming a stable protein complex with them or recognizing substrate epitopes that have been previously phosphorylated by an alternative protein kinase in a process known as priming phosphorylation. Because GSK3-related kinases may need phospho-primed substrates (35), we also generated several phospho-primed versions of the above peptides. We expressed and purified *Arabidopsis* BIN2 in *Escherichia coli* and performed in vitro protein kinase assays against the peptide substrates listed in Table S1. BIN2 phosphorylated a peptide with a phospho-primed serine residue corresponding to phosphorylated CESA1^{S162} (referred to as +pS162; Fig. 3*A*), but none of the other tested peptides (Fig. 3*B*). Interestingly, an identical peptide sequence with no phosphate (−pS162; Fig. 3*A*) was not phosphorylated by BIN2, suggesting that phosphorylation at CESA1^{S162} was required for substrate identification. To map the BIN2 phosphorylation site in the +pS162 peptide, we synthesized +pS162 peptides in which serine and threonine residues were systematically mutated to alanine, a residue that cannot be phosphorylated (Fig. 3*C*). We then retested whether BIN2 could phosphorylate these peptides by in vitro kinase assays. These assays revealed that BIN2 was unable to phosphorylate the +pS162 T157A variant, but could phosphorylate all other alanine substitution peptides to varying degrees (Fig. 3*C*). We further tested whether acidic amino acid substitutions could mimic the effect of the phosphoserine at CESA1^{S162}, but these peptides were not BIN2 substrates (Fig. S3). These results indicate that BIN2 can phosphorylate a threonine residue corresponding to CESA1^{T157} in CESA1 if it is primed by CESA1^{S162} phosphorylation in vitro.

Point Mutations in CESA1 Render It Insensitive to BIN2 Phosphorylation and Enhance Cell Expansion. To examine the physiological function of the CESA1^{T157} BIN2 phosphorylation site, we generated transgenic *Arabidopsis* lines expressing the *CESA1^{wt}* (A1^{wt}), *CESA1^{T157A}* (A1^{T157A}), or *CESA1^{T157E}* (A1^{T157E}) gene under the control of the native *CESA1* promoter in *cesa1*-null background (*Materials and Methods*). Because *cesa1* null mutants are gametophytic-lethal (4), we transformed segregating heterozygous *cesa1$^{+/-}$* plants and monitored *cesa1* homozygosity via PCR genotyping. Transgenic lines expressing *A1^{wt}* in the *cesa1*-null background were phenotypically indistinguishable from wild-type seedlings in a hypocotyl growth assay (Fig. 4 *A* and *B*). Similarly, *cesa1* seedlings expressing *A1^{T157E}* also did not show any phenotypes that deviated from wild-type seedlings (Fig. 4 *A* and *B*). In contrast, *cesa1* mutant seedlings expressing *A1^{T157A}* were 20–40% longer than *A1^{wt}*-complemented *cesa1* control lines or Col-0 controls (Fig. 4 *A* and *B*). Transcript levels of *CESA1* in all lines were assayed to ensure that the phenotypes were not due to overexpression as a consequence of positional genomic effects (Fig. S4). All *CESA1* transcript levels in the transgenic lines were within 1.5-fold levels of the expression in wild-type seedlings (Fig. S4), indicating that the growth differences between the lines are likely not due to differences in *CESA1* expression (as discussed in the previous section). These results indicate that the inability of BIN2 to phosphorylate *A1^{T157A}* could enhance cell expansion. To test this hypothesis, we introgressed *bin2-1* into the *A1^{T157A}*-expressing *cesa1* mutants. Indeed, we found that both homozygous and heterozygous *bin2-1* mutants containing the *A1^{T157A}* mutant in the *cesa1*-null background produced significantly longer hypocotyls than the *bin2-1* control seedlings (Fig. 4 *C* and *D*), suggesting that *A1^{T157A}* partially complements the *bin2-1* mutant hypocotyl growth phenotype.

BIN2-Insensitive CESA1 Mutants Exhibit Increased CSC Activity. To assess further whether the increased seedling growth of *A1^{T157A}*

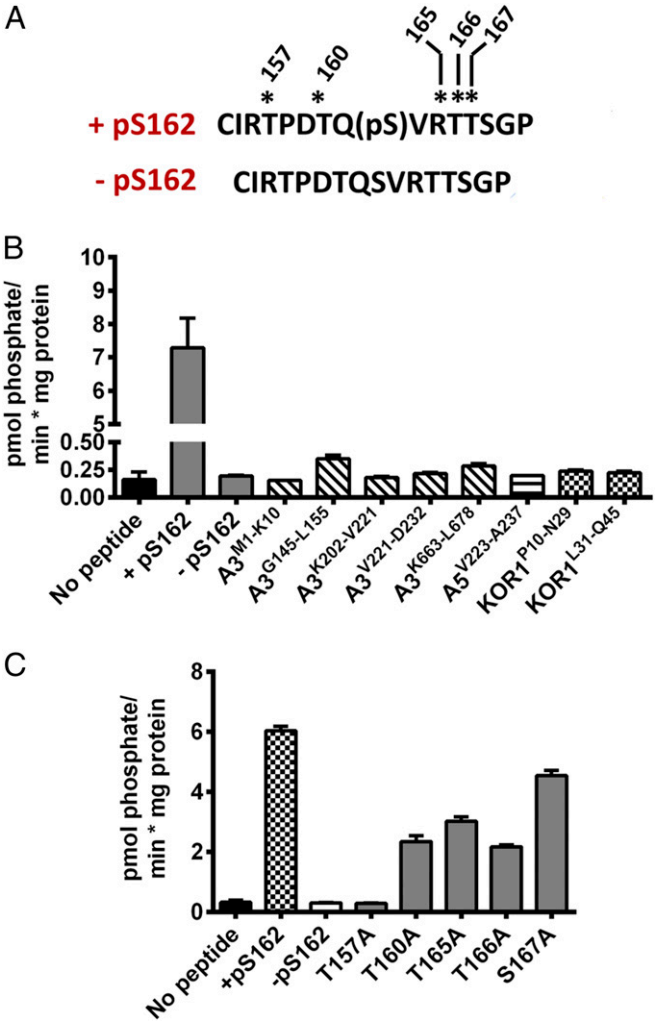

Fig. 3. BIN2 can phosphorylate CESA1 in vitro. Recombinant *Arabidopsis* BIN2 was assayed using a series of peptides by in vitro kinase assays. (*A*) Region of *Arabidopsis* CESA1 that is phosphorylated is shown with the position of the +pS162 and its unphosphorylated counterpart (−pS162) indicated. Asterisks indicate potential phosphorylation sites in the +pS162 peptide. (*B*) Recombinant BIN2 was screened for activity against synthetic peptides representing experimentally supported phosphorylation sites in *Arabidopsis* CESA1 (gray bars), CESA3 (hatched bars), CESA5 (lined bar), and KOR1 (checked bars). (*C*) Synthetic peptides containing alanine substitutions at all possible S/T residues in the +pS162 peptide were assayed as substrates for recombinant BIN2. All assays were repeated at least two times in triplicates. Error bars represent SEM (n = 3).

mutants corresponded to enhanced CSC activity, we introgressed *YFP-CESA6* into the *A1^{T157A}*-expressing *cesa1 bin2-1* double mutant. Due to the fact that *bin2-1* homozygotes display a drastically reduced seed set, seedlings were genotyped after imaging to verify the *bin2-1* genotype. As demonstrated in Fig. 4*E*, the CSCs (YFP-CESA6) moved significantly faster in *bin2-1 cesa1* seedlings that expressed *A1^{T157A}* compared with the CSC speeds in the *bin2-1 cesa1* seedlings that expressed *A1^{wt}*. These results indicate that the A1^{T157A} mutant is not susceptible to the enhanced BIN2-mediated phosphorylation in *bin2-1*, corroborating the hypothesis that BIN2 phosphorylates CESA1, decreases CSC activity, and thus reduces cellulose biosynthesis. Additionally, transgenic plants expressing only the *A1^{T157A}* mutant exhibited faster CSC speeds than wild-type controls (Fig. 4*E*). Defects in secretion of the CSCs also affect cellulose synthesis (36). To assess whether the inability of BIN2 to phosphorylate CESA1 also resulted in trafficking

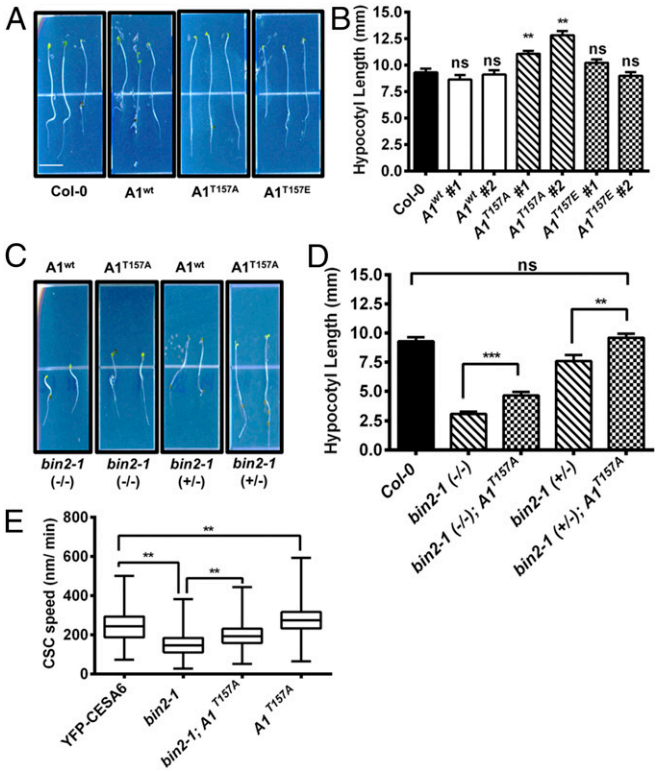

Fig. 4. Mutations of BIN2-targeted CESA1 phosphorylation sites restore growth and CSC velocity in *bin2-1*. *Arabidopsis cesa1*-null mutants were transformed with $CESA1^{wt}$ or $CESA1^{T157}$ phosphorylation site mutants, and the growth behavior of these mutants was examined in 5-d-old dark-grown hypocotyls compared with wild-type Col-0 controls. (*A*) Representative images of $CESA1^{T157A}$ and $CESA1^{T157E}$ phosphorylation site mutants compared with wild-type Col-0 seedlings or *cesa1*-null mutants transformed with $CESA1^{wt}$. (*B*) Quantification of hypocotyl lengths in seedlings from *A*. The means and SEM are presented as in Fig. 1*B*. One-way ANOVA revealed a significant difference: $F(6, 518) = 16.32$ (**$P < 0.01$; $n = 58–103$). ns, not significant from wild-type control by Tukey post hoc analysis. The $CESA1^{T157A}$ mutant was introgressed into a segregating population of the *bin2-1* mutant to determine if $CESA1^{T157A}$ could partially complement *bin2-1*. (*C*) Representative images of *bin2-1* (+/–) or *bin2-1* (–/–) plants with or without $CESA1^{T157A}$. (*D*) Quantification of hypocotyl lengths from *C*. Error bars represent SEM ($n = 19–30$). One-way ANOVA revealed a significant difference: $F(4, 198) = 34.26$. Multiple Student's *t* tests were performed against the indicated conditions (**$P < 0.01$, ***$P < 0.005$). ns, not significant. (*E*) CSC velocities were measured in the *bin2-1* background with or without $CESA1^{T157A}$ and in the $CESA1^{T157A}$ mutant by spinning disk microscopy. These results were compared with *YFP-CESA6* control CSC velocities. Error bars represent minimum and maximum values ($n = 320–1,784$ complexes). One-way ANOVA revealed a significant difference: $F(3, 4,379) = 1057$ (**$P <$ 0.01 by Tukey post hoc analysis between the indicated conditions).

defects, we performed fluorescence recovery after photobleaching experiments (19). We did not find any differences in YFP-CESA6 fluorescence recovery rates between the *bin2-1* $A1^{wt}$ (1.85 ± 0.75 insertions per hour and square micrometer; five seedlings, 17 cells) and the *bin2-1* $A1^{T157A}$ mutant (1.80 ± 0.78 insertions per hour and square micrometer; three seedlings, nine cells), indicating that the BIN2 is not having any major effects on the secretion of CESAs to the plasma membrane. To determine whether these alterations in CSC speed paralleled changes in cellulose deposition, we measured the crystalline cellulose contents of *bin2-1* dark-grown seedlings with or without the expression of $A1^{T157A}$. This experiment revealed that in both homozygous and heterozygous *bin2-1* mutants, crystalline cellulose content was increased in genetic backgrounds that contained $A1^{T157A}$ (Fig. S5). These observations are again consistent with the hypothesis that BIN2 phosphorylates residue T157 in CESAl to regulate cellulose biosynthesis negatively in *Arabidopsis*.

Discussion

Although many recent genetic and cell biological studies continue to define the components of the CSC (e.g., ref. 28), regulatory aspects of the complex are largely unresolved. In this study, we demonstrate that BIN2 kinase, which is transcriptionally coregulated with genes known to encode components of the CSC, can directly and uniquely phosphorylate *Arabidopsis* CESA1 in a priming phosphorylation-dependent manner.

Phosphoproteomic surveys in *Arabidopsis* (29–32), as well as in other plant species (37), indicate that CESA proteins are highly phosphorylated at a number of sites clustered in the N terminus and catalytic loop regions, and that these modifications might functionally regulate CSC activity. Indeed, mutations of CESA1 and CESA3 phosphorylation sites can influence the bidirectional motility of CSCs in *Arabidopsis* (33, 34). Similarly, phosphorylation of CESA5 regulates CSC speed in response to red light/far-red light in a phytochrome-dependent manner (14), suggesting that light quality influences CSC activity. Finally, studies of *Arabidopsis* CesA7 phosphorylation suggest that phosphorylation within the CesA7 N terminus potentially regulates the stability of CesA7 during development (38). Although these studies corroborated that CESA phosphorylation influences CSC activity, the identities of the corresponding kinases have remained unknown.

Priming phosphorylation has been described previously in metazoan and fungal systems by GSK3-like kinases (39–41). Typically, these phosphorylation events occur in the consensus phosphorylation sequence S/T-X-X-X-pS/pT-P, and this sequence is present around the T157 CESA1 in *Arabidopsis* and conserved across CESA1 orthologs in many plant species (Fig. S6). Although several BIN2 substrates have been identified in *Arabidopsis* (42–51), further analyses have revealed that these substrates associate with BIN2 in stable complexes during phosphorylation events and do not require priming phosphorylation. Hence, the CESA1 BIN2 phosphorylation represents a pioneering example of priming phosphorylation in plant systems. Nevertheless, it will be important to identify the protein kinase that catalyzes CesA1 phosphorylation at S162. Additionally, it is important to emphasize that the in vivo T157 phosphorylation event was not specifically observed by biochemical means in this study. The T157 phosphorylation site has been observed in a previous large-scale phosphoproteomic survey (52), suggesting that this phosphorylation site can be phosphorylated in vivo. It will be important in the future to develop methods that allow for the specific in vivo investigation of this and other CSC-related phosphorylation sites, but we would also highlight that genetic experiments presented here support a role of the BIN2 phosphorylated T157 site in the regulation of CSC speed and cell expansion. Such in vivo studies will help us to understand more fully the regulatory controls that influence cellulose biosynthesis.

Plant growth is essentially mediated by two basic processes: cell division and cell expansion. Both phytohormones and cell wall polysaccharide biosynthesis have been demonstrated to participate in these basic developmental processes (3, 4, 13, 53, 54). For example, BR biosynthesis or signaling defects lead to decreased cell expansion, which also may be seen in cellulose biosynthesis mutants (3, 4, 9, 53, 55, 56). However, direct links between these processes have remained scarce. In this paper, we outline a mechanism by which BR signaling can modulate CSC activity, and thus plant biomass production. In the absence of BR, BIN2 is active and phosphorylates CESA1, thereby reducing CSC activity (Fig. 5). When BIN2 is inhibited, or when BR is added, BIN2 becomes inactive and degraded, the CSC is activated, and cellulose synthesis increases (Fig. 5). Our finding that BIN2 directly phosphorylates CESA1, and that this phosphorylation event

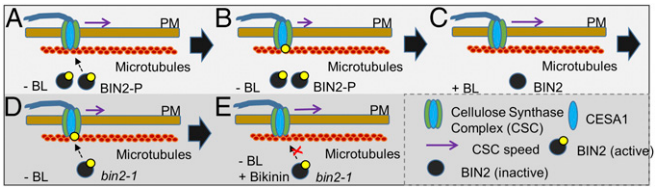

Fig. 5. BIN2 regulates cellulose synthesis activity in *Arabidopsis*. (*A*) Without BRs (−BL), BIN2 is phosphorylated, and thus active. (*B*) Under these conditions, BIN2 phosphorylates CESA1, which, in turn, changes the speed, and thus the activity, of the CSC. (*C*) When BL is added (+BL), BIN2 becomes dephosphorylated by BSU1, which leads to CSC activation. (*D* and *E*) BIN2 activation may be inhibited by BK (GSK3 inhibitor), which leads to reduced BIN2 activity and activation of the CSC.

changes the CSC activity, reveals a prominent protein kinase as a key regulator of cellulose synthesis and directly connects an important hormone signal transduction pathway with a fundamental process in plant growth and development.

Materials and Methods

Growth Conditions. *A. thaliana* (Col-0) plants were germinated and grown as described by Persson et al. (22). Dark-grown seedlings were grown on Murashige and Skoog (MS) agar without sucrose in darkness at 22 °C for 7 d. For small-molecule treatments, Col-0, *det2-1*, and *bin2-1* seedlings were grown on 1/2× MS media in the dark for 5 d. Hypocotyls were collected and placed in 1/2× MS liquid media with 10 nM brassinolide or 5 μM bikinin and incubated on a rotating table for 30 min. Treated hypocotyls were filtered to remove media, immediately frozen in liquid nitrogen, and stored at –80 °C until further use. For cellulose quantification experiments, the seed coats were removed.

Recombinant Purification of BIN2 Kinase. The *BIN2* gene was amplified by PCR from *Arabidopsis* inflorescence cDNA using gene-specific primers [*BIN2* forward (F) and *BIN2* reverse (R); Table S2] and Phusion DNA polymerase (ThermoFisher Scientific), and were cloned into the pENTR-D-TOPO vector (Life Technologies). The *BIN2* ORF was transferred from pENTR-D-TOPO to the pET60-DEST plasmid (Novagen) using LR Clonase II Enzyme Mix (Life Technologies), and then transformed into *E. coli* BL21* cells (Life Technologies). Cell were grown at 37 °C to an OD_{600} of 0.6–0.8 and then induced with 0.5 mM isopropyl-β-D-thiogalactopyranoside for 4 h at 37 °C, and the cells were collected by centrifugation and stored at –80 °C until further use.

Bacterial cells were suspended in buffer A [20 mM Tris·HCl (pH 7.5), 300 mM NaCl, 10 mM $MgCl_2$, and 20 mM imidazole] containing Roche EDTA-free protease inhibitors and lysed with an Avestin Emulsiflex C3 homogenizer (Avestin) at 20,000 psi. The insoluble material was removed by centrifugation at 120,000 × *g* for 1 h at 4 °C, and the supernatant was applied to a 1-mL nickel-nitrilotriacetic acid (Ni-NTA) agarose column equilibrated in buffer A. The column was washed with 500 mL of buffer A and eluted with 10 mL of 20 mM Tris·HCl (pH 7.0), 300 mM NaCl, 10 mM $MgCl_2$, and 350 mM imidazole. The Ni-NTA eluate fraction was then applied to 0.5 mL of glutathione-Sepharose 4B (GE Healthcare) and incubated on a rocker table at 4 °C for 1 h. The resin was loaded into a column, washed with 250 mL of wash buffer, and then eluted in 8 × 1-mL fractions with buffer A containing 10 mM reduced glutathione and adjusted to pH 7.0. Purity of the purified recombinant protein was assessed by SDS/PAGE analysis.

Protein Kinase Assays. In vitro kinase assays were conducted in 50-μL reactions containing kinase buffer [25 mM 3-(*N*-morpholino)propanesulfonic acid–NaOH (pH 7.0), 10 mM $MgCl_2$, and 100 μM ATP containing 1,000 dpm/pmol γ-[^{32}P]-ATP]. Peptide substrates were included in the assays at a concentration of 100 μM, and the assays were initiated by the addition of recombinant protein kinase. Samples were incubated at 37 °C for 30 min; then, a 25-μL aliquot was removed from each reaction, spotted on P81 phosphocellulose paper, dried for 2 min, and placed in 75 mM phosphoric acid. The filters were washed three times for 5 min in 75 mM phosphoric acid and 5 min in 95% (vol/vol) EtOH, and then dried. Incorporation of ^{32}P was monitored by scintillation counting using a PerkinElmer TriCarb 2810TR scintillation counter.

Confocal Microscopy. Transgenic lines expressing *pCESA6::YFP-CESA6* in the *prc1-1* mutant background have been described previously (6). Seedlings for image analysis were grown in the dark on MS-agar media at 22 °C for 4 d. Seedlings were imaged using a CSU-W1 spinning disk head (Yokogawa) mounted to an inverted Nikon Ti-E microscope equipped with a 100× oil-immersion objective (Apo total internal reflection fluorescence, N.A. = 1.49) and a deep-cooled iXon Ultra 888 EM-CCD camera (Andor Technology) controlled by Metamorph software. Photobleaching was achieved using an Andor FRAPPA scanning instrument attached to the system above (36). For CSC motility assays, seedlings were imaged with an 800-ms exposure every 10 s for 5–8 min.

The recorded time-lapse movies were corrected for drift and bleaching using the ImageJ (NIH) plug-ins "stackreg," "subtract background," and "bleach correction" with default settings. In cases of weak intensity, we further applied the "walking average" plug-in. Velocities were analyzed using the "kymograph evaluation" plug-in of the free tracking software FIESTA (57). More than 100 kymographs were analyzed per cell, and the velocities of CESAs were determined by approximating the slopes of their trajectories with a straight line.

Complementation Experiments. To generate plant transformation vectors containing *CESA1* or phosphorylation site mutants under the native *CESA1* promoter, the *pCESA1*/pDONR P4-P1r vector, the respective *CESA1* entry clone, and a Nos-terminator/pDONR P2r-P3 vector (58) were combined in the presence of the pH7m34GW multisite gateway vector (59) and LR Clonase II Plus (Invitrogen). Constructs were transformed into a heterozygous *cesa1* T-DNA insertional mutant line (SALK_092266) by the standard floral dip method (60).

An *Arabidopsis* mutant harboring a T-DNA insertion in *CESA1* exon 14 was obtained from the Arabidopsis Biological Resource Center (https://abrc.osu.edu/), and individual seedlings were genotyped by PCR using the primers SALK_092266 LP, SALK_092266 RP, and LBb1.3 shown in Table S2. As expected, no homozygous plants were obtained due to the previously described lethality of *cesa1*-null mutations (3, 4). To circumvent this issue, primary transformants containing the appropriate *pCESA1::CESA1* cDNA construct were identified by PCR genotyping using the Hph F and Hph R primers listed in Table S2, which amplify the hygromycin resistance cassette associated with the pH7m34GW transformation vector. A second set of genotyping primers was designed to amplify selectively the genomic *CESA1* sequences surrounding the SALK_092266 T-DNA insertion site (*CESA1* intron 13 F and *CESA1* 3′UTR R; Table S2). These primers were used in conjunction with the LBb1.3 primer to identify primary *pCESA1::CESA1* cDNA transformants that were heterozygous for the SALK_092266 T-DNA insertion. These plants were allowed to self-fertilize, and the progeny of subsequent generations were analyzed by PCR genotyping in a similar manner to identify plants containing a copy of the *pCESA1::CESA1* cDNA complement construct as well as a homozygous T-DNA insertion in the endogenous copy of *CESA1*. These transgenic lines were subsequently crossed to the previously described *YFP-CESA6* reporter line (6) and/or the *bin2-1* mutant (9) to generate the appropriate transgenic lines. *Arabidopsis* mutants harboring *YFP-CESA6* in the *prc1-1* background were genotyped using *YFP* genotyping F and *CESA6* genotyping R primers. *Arabidopsis bin2-1* lines were genotyped using BIN2 XhoI F and BIN2 XhoI R (Table S2), and subsequent restriction digest of amplified products with XhoI was required to identify heterozygous and homozygous mutants for the *bin2-1* point mutation (9).

RNA Isolation, cDNA Synthesis, and Quantitative RT-PCR. RNA was isolated using the PureLink Plant RNA Kit according to the manufacturer's instructions (ThermoFisher Scientific). First-strand cDNA was synthesized using the Invitrogen SuperScript III First-Strand Synthesis System according to the manufacturer's protocol (ThermoFisher Scientific). Real-time quantitative PCR was performed using BioRad iTaq Universal SYBR Green Supermix. PCR reactions were performed on a BioRad CFX 96 Real-Time System using suggested Universal SYBR Green Supermix conditions, and data analysis was performed using Prism software (GraphPad). The following genes were used as amplification references: *GLYCERALDEHYDE-3-PHOSPHATE DEHYDROGENASE* (*GAPDH*; At1g13440; Fig. S1*A*), *ACTIN2* (*ACT2*; At3g18780; Fig. S4), *UBIQUITIN CONJUGATING ENZYME 21* (*UBC21*; At5g25760; Fig. S1*B*). The primer sequences for these reference genes and all transcripts assayed in this study are included in Table S2.

Cellulose Measurement. Crystalline cellulose content was measured by previously described methods (61), with minor modifications (62). More detailed materials and methods are available in *SI Materials and Methods*.

ACKNOWLEDGMENTS. We thank Dr. Christopher Kesten and Dr. Edwin Lampugnani for experimental assistance and critical evaluation of this manuscript. C.S.-R. and S.P. were financially supported by the Max-Planck Gesellschaft. S.P. was supported by a R@MAP Professorship at the University of Melbourne. K.K. and I.S.W. are supported by startup funds from the Biochemistry and Molecular Biology Department at the University of Nevada,

Reno as well as the National Science Foundation (Grant IOS 1449068) and a Nevada Agricultural Experiment Station Award (NEV00382). Support was also received from the Energy Biosciences Institute at the University of California, Berkeley and the Philomathia Foundation.

1. Somerville C, et al. (2004) Toward a systems approach to understanding plant cell walls. *Science* 306(5705):2206–2211.
2. Schneider R, Hanak T, Persson S, Voigt CA (2016) Cellulose and callose synthesis and organization in focus, what's new? *Curr Opin Plant Biol* 34:9–16.
3. Desprez T, et al. (2007) Organization of cellulose synthase complexes involved in primary cell wall synthesis in Arabidopsis thaliana. *Proc Natl Acad Sci USA* 104(39): 15572–15577.
4. Persson S, et al. (2007) Genetic evidence for three unique components in primary cell-wall cellulose synthase complexes in Arabidopsis. *Proc Natl Acad Sci USA* 104(39): 15566–15571.
5. Diotallevi F, Mulder B (2007) The cellulose synthase complex: A polymerization driven supramolecular motor. *Biophys J* 92(8):2666–2673.
6. Paredez AR, Somerville CR, Ehrhardt DW (2006) Visualization of cellulose synthase demonstrates functional association with microtubules. *Science* 312(5779):1491–1495.
7. Kim TW, Wang ZY (2010) Brassinosteroid signal transduction from receptor kinases to transcription factors. *Annu Rev Plant Biol* 61:681–704.
8. Wang ZY, Bai MY, Oh E, Zhu JY (2012) Brassinosteroid signaling network and regulation of photomorphogenesis. *Annu Rev Genet* 46:701–724.
9. Li J, Nam KH (2002) Regulation of brassinosteroid signaling by a GSK3/SHAGGY-like kinase. *Science* 295(5558):1299–1301.
10. He JX, Gendron JM, Yang Y, Li J, Wang ZY (2002) The GSK3-like kinase BIN2 phosphorylates and destabilizes BZR1, a positive regulator of the brassinosteroid signaling pathway in Arabidopsis. *Proc Natl Acad Sci USA* 99(15):10185–10190.
11. Wang ZY, et al. (2002) Nuclear-localized BZR1 mediates brassinosteroid-induced growth and feedback suppression of brassinosteroid biosynthesis. *Dev Cell* 2(4): 505–513.
12. Peng P, Yan Z, Zhu Y, Li J (2008) Regulation of the Arabidopsis GSK3-like kinase BRASSINOSTEROID-INSENSITIVE 2 through proteasome-mediated protein degradation. *Mol Plant* 1(2):338–346.
13. Sánchez-Rodríguez C, Rubio-Somoza I, Sibout R, Persson S (2010) Phytohormones and the cell wall in Arabidopsis during seedling growth. *Trends Plant Sci* 15(5):291–301.
14. Bischoff V, et al. (2011) Phytochrome regulation of cellulose synthesis in Arabidopsis. *Curr Biol* 21(21):1822–1827.
15. Xie L, Yang C, Wang X (2011) Brassinosteroids can regulate cellulose biosynthesis by controlling the expression of CESA genes in Arabidopsis. *J Exp Bot* 62(13):4495–4506.
16. Li J, Nagpal P, Vitart V, McMorris TC, Chory J (1996) A role for brassinosteroids in light-dependent development of Arabidopsis. *Science* 272(5260):398–401.
17. De Rybel B, et al. (2009) Chemical inhibition of a subset of Arabidopsis thaliana GSK3-like kinases activates brassinosteroid signaling. *Chem Biol* 16(6):594–604.
18. DeBolt S, Gutierrez R, Ehrhardt DW, Somerville C (2007) Nonmotile cellulose synthase subunits repeatedly accumulate within localized regions at the plasma membrane in Arabidopsis hypocotyl cells following 2,6-dichlorobenzonitrile treatment. *Plant Physiol* 145(2):334–338.
19. Gutierrez R, Lindeboom JJ, Paredez AR, Emons AM, Ehrhardt DW (2009) Arabidopsis cortical microtubules position cellulose synthase delivery to the plasma membrane and interact with cellulose synthase trafficking compartments. *Nat Cell Biol* 11(7): 797–806.
20. Gu Y, et al. (2010) Identification of a cellulose synthase-associated protein required for cellulose biosynthesis. *Proc Natl Acad Sci USA* 107(29):12866–12871.
21. Bringmann M, et al. (2012) POM-POM2/cellulose synthase interacting1 is essential for the functional association of cellulose synthase and microtubules in Arabidopsis. *Plant Cell* 24(1):163–177.
22. Persson S, Wei H, Milne J, Page GP, Somerville CR (2005) Identification of genes required for cellulose synthesis by regression analysis of public microarray data sets. *Proc Natl Acad Sci USA* 102(24):8633–8638.
23. Ruprecht C, et al. (2016) FamNet: A framework to identify multiplied modules driving pathway expansion in plants. *Plant Physiol* 170(3):1878–1894.
24. Vain T, et al. (2014) The cellulase KORRIGAN is part of the cellulose synthase complex. *Plant Physiol* 165(4):1521–1532.
25. Mansoori N, et al. (2014) KORRIGAN1 interacts specifically with integral components of the cellulose synthase machinery. *PLoS One* 9(11):e112387.
26. Roudier F, et al. (2005) COBRA, an Arabidopsis extracellular glycosyl-phosphatidyl inositol-anchored protein, specifically controls highly anisotropic expansion through its involvement in cellulose microfibril orientation. *Plant Cell* 17(6):1749–1763.
27. Liu L, et al. (2013) Brittle Culm1, a COBRA-like protein, functions in cellulose assembly through binding cellulose microfibrils. *PLoS Genet* 9(8):e1003704.
28. Endler A, et al. (2015) A mechanism for sustained cellulose synthesis during salt stress. *Cell* 162(6):1353–1364.
29. Nühse TS, Stensballe A, Jensen ON, Peck SC (2004) Phosphoproteomics of the Arabidopsis plasma membrane and a new phosphorylation site database. *Plant Cell* 16(9): 2394–2405.
30. Nühse TS, Bottrill AR, Jones AM, Peck SC (2007) Quantitative phosphoproteomic analysis of plasma membrane proteins reveals regulatory mechanisms of plant innate immune responses. *Plant J* 51(5):931–940.
31. Nakagami H, et al. (2010) Large-scale comparative phosphoproteomics identifies conserved phosphorylation sites in plants. *Plant Physiol* 153(3):1161–1174.
32. Jones DM, et al. (2016) The emerging role of protein phosphorylation as a critical regulatory mechanism controlling cellulose biosynthesis. *Front Plant Sci* 7:684.
33. Chen S, Ehrhardt DW, Somerville CR (2010) Mutations of cellulose synthase (CESA1) phosphorylation sites modulate anisotropic cell expansion and bidirectional mobility of cellulose synthase. *Proc Natl Acad Sci USA* 107(40):17188–17193.
34. Chen S, et al. (2016) Anisotropic cell expansion is affected through the bidirectional mobility of cellulose synthase complexes and phosphorylation at two critical residues on CESA3. *Plant Physiol* 171(1):242–250.
35. Chu B, Soncin F, Price BD, Stevenson MA, Calderwood SK (1996) Sequential phosphorylation by mitogen-activated protein kinase and glycogen synthase kinase 3 represses transcriptional activation by heat shock factor-1. *J Biol Chem* 271(48): 30847–30857.
36. Luo Y, et al. (2015) V-ATPase activity in the TGN/EE is required for exocytosis and recycling in Arabidopsis. *Nat Plants* 1:15094.
37. Facette MR, Shen Z, Björnsdóttir FR, Briggs SP, Smith LG (2013) Parallel proteomic and phosphoproteomic analyses of successive stages of maize leaf development. *Plant Cell* 25(8):2798–2812.
38. Taylor NG (2007) Identification of cellulose synthase AtCesA7 (IRX3) in vivo phosphorylation sites–a potential role in regulating protein degradation. *Plant Mol Biol* 64(1-2):161–171.
39. Millet C, et al. (2009) A negative feedback control of transforming growth factor-beta signaling by glycogen synthase kinase 3-mediated Smad3 linker phosphorylation at Ser-204. *J Biol Chem* 284(30):19808–19816.
40. Takeo S, et al. (2012) Shaggy/glycogen synthase kinase 3β and phosphorylation of Sarah/regulator of calcineurin are essential for completion of Drosophila female meiosis. *Proc Natl Acad Sci USA* 109(17):6382–6389.
41. Al-Zain A, Schroeder L, Sheglov A, Ikui AE (2015) Cdc6 degradation requires phosphodegron created by GSK-3 and Cdk1 for SCF^{Cdc4} recognition in Saccharomyces cerevisiae. *Mol Biol Cell* 26(14):2609–2619.
42. Peng P, Zhao J, Zhu Y, Asami T, Li J (2010) A direct docking mechanism for a plant GSK3-like kinase to phosphorylate its substrates. *J Biol Chem* 285(32):24646–24653.
43. Kim TW, Michniewicz M, Bergmann DC, Wang ZY (2012) Brassinosteroid regulates stomatal development by GSK3-mediated inhibition of a MAPK pathway. *Nature* 482(7385):419–422.
44. Gudesblat GE, et al. (2012) SPEECHLESS integrates brassinosteroid and stomata signalling pathways. *Nat Cell Biol* 14(5):548–554.
45. Tong H, et al. (2012) DWARF AND LOW-TILLERING acts as a direct downstream target of a GSK3/SHAGGY-like kinase to mediate brassinosteroid responses in rice. *Plant Cell* 24(6):2562–2577.
46. Ye H, Li L, Guo H, Yin Y (2012) MYBL2 is a substrate of GSK3-like kinase BIN2 and acts as a corepressor of BES1 in brassinosteroid signaling pathway in Arabidopsis. *Proc Natl Acad Sci USA* 109(49):20142–20147.
47. Zhang D, et al. (2014) Transcription factor HAT1 is phosphorylated by BIN2 kinase and mediates brassinosteroid repressed gene expression in Arabidopsis. *Plant J* 77(1): 59–70.
48. Cho H, et al. (2014) A secreted peptide acts on BIN2-mediated phosphorylation of ARFs to potentiate auxin response during lateral root development. *Nat Cell Biol* 16(1):66–76.
49. Cai Z, et al. (2014) GSK3-like kinases positively modulate abscisic acid signaling through phosphorylating subgroup III SnRK2s in Arabidopsis. *Proc Natl Acad Sci USA* 111(26):9651–9656.
50. Bernardo-García S, et al. (2014) BR-dependent phosphorylation modulates PIF4 transcriptional activity and shapes diurnal hypocotyl growth. *Genes Dev* 28(15): 1681–1694.
51. Hu Y, Yu D (2014) BRASSINOSTEROID INSENSITIVE2 interacts with ABSCISIC ACID INSENSITIVE5 to mediate the antagonism of brassinosteroids to abscisic acid during seed germination in Arabidopsis. *Plant Cell* 26(11):4394–4408.
52. Mattei B, Spinelli F, Pontiggia D, De Lorenzo G (2016) Comprehensive analysis of the membrane phosphoproteome regulated by oligogalacturonides in Arabidopsis thaliana. *Front Plant Sci* 7:1107.
53. Arioli T, et al. (1998) Molecular analysis of cellulose biosynthesis in Arabidopsis. *Science* 279(5351):717–720.
54. Miart F, et al. (2014) Spatio-temporal analysis of cellulose synthesis during cell plate formation in Arabidopsis. *Plant J* 77(1):71–84.
55. Li J, Chory J (1997) A putative leucine-rich repeat receptor kinase involved in brassinosteroid signal transduction. *Cell* 90(5):929–938.
56. Clouse SD, Langford M, McMorris TC (1996) A brassinosteroid-insensitive mutant in Arabidopsis thaliana exhibits multiple defects in growth and development. *Plant Physiol* 111(3):671–678.
57. Ruhnow F, Zwicker D, Diez S (2011) Tracking single particles and elongated filaments with nanometer precision. *Biophys J* 100(11):2820–2828.
58. Karimi M, Depicker A, Hilson P (2007) Recombinational cloning with plant gateway vectors. *Plant Physiol* 145(4):1144–1154.
59. Karimi M, De Meyer B, Hilson P (2005) Modular cloning in plant cells. *Trends Plant Sci* 10(3):103–105.
60. Clough SJ, Bent AF (1998) Floral dip: A simplified method for Agrobacterium-mediated transformation of Arabidopsis thaliana. *Plant J* 16(6):735–743.
61. Updegraff DM (1969) Semimicro determination of cellulose in biological materials. *Anal Biochem* 32(3):420–424.
62. Villalobos JA, Yi BR, Wallace IS (2015) 2-Fluoro-L-fucose is a metabolically incorporated inhibitor of plant cell wall polysaccharide fucosylation. *PLoS One* 10(9): e0139091.